



Published in final edited form as:

Cell Rep. 2017 October 24; 21(4): 1009–1020. doi:10.1016/j.celrep.2017.10.002.

## Dendritic Cell Amiloride-Sensitive Channels Mediate Sodium-Induced Inflammation and Hypertension

Natalia R. Barbaro<sup>1,4</sup>, Jason D. Foss<sup>1,4</sup>, Dmytro O. Kryshchal<sup>1</sup>, Nikita Tsyba<sup>1</sup>, Shivani Kumaresan<sup>1</sup>, Liang Xiao<sup>1</sup>, Raymond L. Mernaugh<sup>3</sup>, Hana A. Itani<sup>1</sup>, Roxana Loperena<sup>2</sup>, Wei Chen<sup>1</sup>, Sergey Dikalov<sup>1</sup>, Jens M. Titze<sup>1</sup>, Bjorn C. Knollmann<sup>1</sup>, David G. Harrison<sup>1,2</sup>, and Annet Kirabo<sup>1,2,5,6,\*</sup>

<sup>1</sup>Division of Clinical Pharmacology, Department of Medicine, Vanderbilt University Medical Center, Nashville, TN, USA

<sup>2</sup>Department of Molecular Physiology and Biophysics, Vanderbilt University, Nashville, TN, USA

<sup>3</sup>Department of Biochemistry, Vanderbilt University, Nashville, TN, USA

### SUMMARY

Sodium accumulates in the interstitium and promotes inflammation through poorly defined mechanisms. We describe a pathway by which sodium enters dendritic cells (DCs) through amiloride-sensitive channels including the alpha and gamma subunits of the epithelial sodium channel and the sodium hydrogen exchanger 1. This leads to calcium influx via the sodium calcium exchanger, activation of protein kinase C (PKC), phosphorylation of p47<sup>phox</sup>, and association of p47<sup>phox</sup> with gp91<sup>phox</sup>. The assembled NADPH oxidase produces superoxide with subsequent formation of immunogenic isolevuglandin (IsoLG)-protein adducts. DCs activated by excess sodium produce increased interleukin-1 $\beta$  (IL-1 $\beta$ ) and promote T cell production of cytokines IL-17A and interferon gamma (IFN- $\gamma$ ). When adoptively transferred into naive mice, these DCs prime hypertension in response to a sub-pressor dose of angiotensin II. These findings provide a mechanistic link between salt, inflammation, and hypertension involving increased oxidative stress and IsoLG production in DCs.

### In Brief

This is an open access article under the CC BY-NC-ND license (<http://creativecommons.org/licenses/by-nc-nd/4.0/>).

\*Correspondence: [annet.kirabo@vanderbilt.edu](mailto:annet.kirabo@vanderbilt.edu).

<sup>4</sup>These authors contributed equally

<sup>5</sup>Twitter: @annetkiraboc1

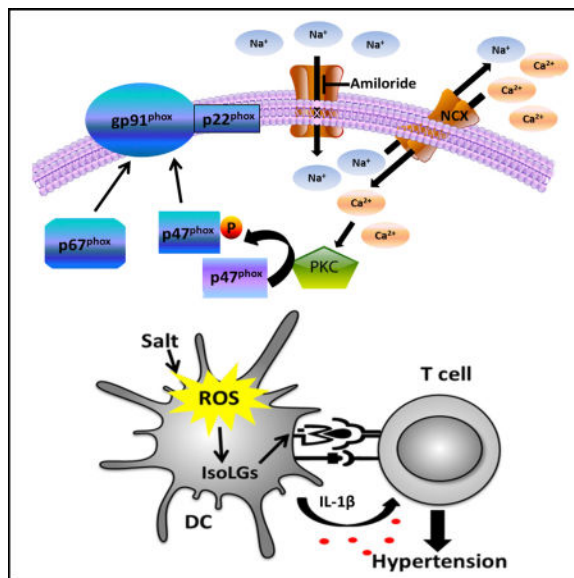
<sup>6</sup>Lead Contact

### SUPPLEMENTAL INFORMATION

Supplemental Information includes one figure and one table and can be found with this article online at <https://doi.org/10.1016/j.celrep.2017.10.002>.

### AUTHOR CONTRIBUTIONS

N.R.B., J.D.F., D.O.K., N.T., S.K., L.X., R.L.M., H.A.I., R.L., W.C., S.D., and A.K. performed the experiments. N.R.B., J.M.T., D.G.H., and A.K. conceived the research program, designed experiments, and wrote the manuscript. J.M.T., B.C.K., A.K., and D.G.H. edited and approved the manuscript. N.R.B., D.G.H., and K.A. obtained funding for the manuscript.



Barbaro et al. describe a pathway by which increased extracellular sodium activates dendritic cells. This pathway potentially explains the link between excessive salt intake, inflammation, and high blood pressure.

## INTRODUCTION

Hypertension affects over 1 billion people worldwide and is a major risk factor for death and disability (Kearney et al., 2005; Murray and Lopez, 2013). The etiology of most cases of hypertension is unknown and a large portion of hypertensive patients has elevated blood pressure despite extensive drug therapy (Benjamin et al., 2017). Over the past several years, it has become increasingly clear that inflammation contributes to the genesis of hypertension. Our laboratory and others have shown that cells of both the adaptive and innate immune systems contribute to this disease (McMaster et al., 2015). In particular, T cells with an effector phenotype infiltrate the kidneys and perivascular space in response to hypertensive stimuli, release inflammatory cytokines, and promote renal and vascular dysfunction leading to elevated blood pressure (Guzik et al., 2007; Madhur et al., 2010). Deletion of the recombina-activating gene 1 lowers blood pressure and prevents renal injury in rats with salt-sensitive hypertension (Mattson et al., 2013). Humans with hypertension have increased numbers of circulating activated CD8<sup>+</sup> T cells with a senescent phenotype (Youn et al., 2013), and interleukin-17A (IL-17A)-producing CD4<sup>+</sup> T cells are increased in the circulation of humans with hypertension (Itani et al., 2016).

Another factor that contributes to the pathogenesis of hypertension is salt (NaCl). Dietary salt intake is positively correlated with blood pressure, and reductions in salt intake reduce blood pressure and cardiovascular events (Ha, 2014). The mechanisms underlying the relationship between salt and hypertension are not fully understood. Recent work by Titze and colleagues has shown that changes in extra-renal sodium handling can cause accumulation of sodium in the interstitium at levels that exceed that of plasma (Kopp et al., 2013; Machnik et al., 2009; Titze and Machnik, 2010). Using <sup>23</sup>Na MRI, these investigators

showed that blood pressure in humans is positively correlated with both skin and muscle sodium content (Kopp et al., 2013). Recent evidence suggests that these high sodium concentrations can alter immune cell function. Exposure of either mouse macrophages or T cells to high NaCl concentration drives them toward a pro-inflammatory state (Binger et al., 2015; Jantsch et al., 2015; Jörg et al., 2016; Kleinewietfeld et al., 2013; Wu et al., 2013; Zhang et al., 2015). Specifically, elevation of extracellular NaCl promotes production of IL-17A by T cells and salt feeding exacerbates experimental allergic encephalitis, a disease driven by this cytokine. Moreover, high-salt feeding in humans has been linked to increased monocyte numbers and increased plasma IL-23, which, in turn, can sustain IL-17 production by T cells (Yi et al., 2015). Of note, mice lacking IL-17A are partly protected from hypertension, and IL-17A can promote both renal and vascular dysfunction, leading to blood pressure elevation (Chiasson et al., 2011; Madhur et al., 2010; Nguyen et al., 2013).

T cells are activated when antigen-presenting cells, such as dendritic cells (DCs), macrophages, and B cells present antigens recognized by the T cell receptor. We recently elucidated a pathway by which DCs become activated and promote hypertension. We found that experimental hypertension is associated with an increase in NADPH-oxidase-dependent superoxide production in DCs, which leads to formation of highly reactive  $\gamma$ -ketoaldehydes, also known as isoketals or isolevuglandins (IsoLGs) (Kirabo et al., 2014). These rapidly adduct to self-proteins that are processed and presented as neoantigens by DCs, promoting an autoimmune-like state leading to renal and vascular dysfunction and hypertension. Moreover, DCs that accumulate IsoLGs produce large amounts of IL-6, IL-1 $\beta$ , and IL-23, which are known to promote differentiation of naive T cells into pro-inflammatory and pro-hypertensive IL-17A-producing cells (Madhur et al., 2010; Mills, 2008). In the present studies, we show that excessive salt promotes DC activation via increased superoxide production and IsoLG-protein adduct formation. This is due to increased activation of the NADPH oxidase, which is mediated by Ca<sup>2+</sup>/PKC-dependent phosphorylation of p47<sup>phox</sup>.

## RESULTS

### High Salt Activates the NADPH Oxidase in DCs, Leading to Increased Superoxide Production through an Amiloride-Inhibitible Sodium Channel and Sodium-Calcium Exchanger

A predominant source of reactive oxygen species in phagocytic cells like DCs is the NADPH oxidase. We recently found that long-term angiotensin II infusion in mice increases NADPH-oxidase-dependent superoxide production in DCs resulting in the formation of immunogenic IsoLGs (Kirabo et al., 2014). To determine whether high salt affects the DC NADPH oxidase, we isolated splenic DCs from mice and cultured them for 24 hr in either normal-salt (150 mM NaCl) or high-salt media (190 mM NaCl). Exposure to the high-salt media markedly increased DC superoxide production as measured by electron spin resonance (ESR). Co-incubation with the peptide gp91 ds-tat, a competitive inhibitor of NADPH oxidase assembly, prevented the high-salt-induced production of superoxide (Figures 1A and 1B). In addition, we found that increasing extracellular NaCl from 150 to 190 mM increased intracellular sodium as measured by flow cytometry using sodium green (Figures 1C and 1D).

To explore potential mechanisms by which sodium might enter DCs, we initially performed real-time RT-PCR for several known sodium transporters. This revealed mRNA expression of the sodium-potassium chloride cotransporter-1 (NKCC1), sodium hydrogen exchangers (NHE1 and NHE6), the sodium-chloride cotransporter (NCC), the sodium-calcium exchangers (NCX1 and NCX2), and the epithelial sodium channel (ENaC,  $\alpha$  and  $\gamma$  subunits). The  $\beta$  subunit of ENaC was not present (data not shown). High salt did not significantly affect the amount of message observed for any transporter (Figure 1E).

To determine which of the sodium transporters facilitate the high-salt-induced activation of the NADPH oxidase, we pre-incubated mouse DCs with various inhibitors of these transporters and used phosphorylation of p47<sup>phox</sup> as an indicator of NADPH oxidase activation. Compared to normal salt, high salt markedly increased phosphorylation of p47<sup>phox</sup> as determined by western blot. While inhibition of NKCC with furosemide and NCC with hydrochlorothiazide did not have any effect, amiloride, which inhibits both ENaC and NHE, and KB-R7943 mesylate, a selective reverse mode NCX inhibitor, completely prevented the high-salt-induced phosphorylation of p47<sup>phox</sup> (Figure 1F). These results suggest that the effects of salt on DCs leading to phosphorylation of p47<sup>phox</sup> require activity of both NCX and an amiloride-inhibitable sodium channel such as either ENaC or NHE.

In additional experiments, we confirmed by western blot that both the alpha and gamma subunits of ENaC are indeed expressed by DCs (Figure 1G), while the beta subunit is not (data not shown). A key step in assembly of the NADPH oxidase is movement of p47<sup>phox</sup> to the membrane and its docking to gp91<sup>phox</sup>. To determine whether high salt causes assembly of the NADPH oxidase and whether this is mediated via ENaC, we immunoprecipitated gp91<sup>phox</sup> and performed western blots for associated p47<sup>phox</sup>. We found that compared to normal salt, high salt induced a striking association of p47<sup>phox</sup> with gp91<sup>phox</sup> and that this was prevented by co-incubation with amiloride and benzamil (Figure 1H). Since both amiloride and benzamil can also inhibit NHE, we used cariporide, a selective inhibitor of NHE and found that it also prevented the high-salt-induced association of p47<sup>phox</sup> with gp91<sup>phox</sup> (Figure 1I).

To confirm the specific involvement of ENaC in mediating the high-salt-induced activation of NADPH oxidase, we used small interfering RNA (siRNA) to specifically silence expression of  $\alpha$ -ENaC in DCs. As shown in Figure 1J, this approach resulted in a marked reduction of  $\alpha$ -ENaC expression in DCs and prevented association of p47<sup>phox</sup> with gp91<sup>phox</sup> (Figure 1K). Similarly, we achieved a marked siRNA-mediated knockdown of NHE1 (Figure 1L), and this also prevented association of p47<sup>phox</sup> with gp91<sup>phox</sup> (Figure 1M). Collectively, these results suggest that elevated sodium concentrations drive NADPH-oxidase-dependent superoxide production, and this is mediated through both ENaC and NHE.

### **The Salt-Induced Activation of the NADPH Oxidase in DCs Is Calcium and PKC Dependent**

The NADPH oxidase subunit p47<sup>phox</sup> is phosphorylated by calcium-sensitive isoforms of protein kinase C (PKC) (Garcia et al., 1992; Papini et al., 1985). Since KB-R7943 mesylate, a selective reverse mode NCX inhibitor prevented the high-salt-induced phosphorylation of p47<sup>phox</sup> (Figure 1F), we hypothesized that excess sodium would lead to calcium influx and

activation of PKC leading to activation of the NADPH oxidase. Using co-immunoprecipitation, we found that co-incubation with the selective cell permeant calcium chelator 1,2-bis(o-aminophenoxy) ethane-N,N,N',N'-tetraacetic acid (BAPTA-AM) (Figure 2A) or the specific PKC inhibitor calphostin C (Figure 2B) prevented the salt-induced association of p47<sup>phox</sup> with gp91<sup>phox</sup>. In additional experiments, we monitored intracellular Ca<sup>2+</sup> using fluorescence photometry (IonOptix) and found that 15 min of exposure to high salt leads to a marked increase in intracellular calcium (Figures 2C and 2D). Inhibition of the NCX using nickel chloride (NiCl<sub>2</sub>) prevented the salt-induced calcium increase in DCs (Figure 2D). In additional studies, we found that co-treatment with amiloride prevents the high-salt-induced Ca<sup>2+</sup> influx (Figure 2E). These results indicate that high-salt exposure induces assembly of NADPH oxidase in DCs and that this is dependent on calcium entry via the NCX and PKC signaling.

### High-Salt Exposure Activates DCs via Increased Production of Immunogenic IsoLGs

We have previously found that increased superoxide production in DCs is associated with DC activation and the accumulation of IsoLG-protein adducts (Kirabo et al., 2014). Therefore, we cultured mouse splenocytes in normal-salt media (150 mM NaCl), high-salt media (190 mM NaCl), or normal-salt media with mannitol (80 mM) added as an osmotic control for 24 hr and performed flow cytometry using a previously described gating strategy (Figure 3A), which discriminates macrophages from DCs (Jakubzick et al., 2013). Intracellular staining was performed with the single-chain antibody, D11 ScFv, which identifies IsoLG-protein adducts independent of the amino acid backbone (Figures 3B–3E) (Davies et al., 2004). We found that exposure to high salt but not mannitol increases IsoLG-adduct formation in DCs and macrophages (Figures 3B and 3C).

When DCs present antigens, they undergo a maturation process associated with increased expression of co-stimulatory molecules such as the B7 ligands CD80 and CD86, which we have shown to be essential for hypertension (Vinh et al., 2010). Using flow cytometry, we found that exposure to high salt, but not mannitol, increased surface expression of CD86 in DCs (Figure 3D). Likewise, macrophages had increased expression of CD86 in response to high salt but not mannitol (Figure 3E). Expression of CD80 was not different between treatment groups in both DCs (Figure 3F) and macrophages (Figure 3G).

To determine whether the high-salt-induced IsoLG formation is dependent on the NADPH oxidase, we created mice that lack the p22<sup>phox</sup> docking subunit of this enzyme complex in CD11c<sup>+</sup> cells (tg<sup>CD11c-cre</sup>/p22<sup>phoxloxP/loxP</sup>). We used littermates with loxP sites but no Cre recombinase as controls (p22<sup>phoxloxP/loxP</sup>). DCs isolated from these two strains of mice were cultured for 24 hr in either normal salt or high salt, and flow cytometry was performed to determine the presence of IsoLGs. As shown in Figures 3H and 3I, high salt caused an increase in IsoLG-protein adducts in DCs from control mice, but DC-targeted deletion of p22<sup>phox</sup> prevented this salt-induced IsoLG formation. Collectively, these experiments suggest that the high-salt-induced formation of superoxide and IsoLGs in DCs is NADPH oxidase dependent.

An important aspect of DC activation is cytokine production. We isolated DCs from spleens of mice, cultured them in normal or high-salt media, and measured a panel of cytokines

using a Luminex-based assay. We found that high-salt exposure significantly increased DC production of IL-1 $\beta$  (Figure 4A) and that there was a trend for an increase in IL-6 (Figure 4B) and tumor necrosis factor alpha (TNF- $\alpha$ ) (Figure 4C). A complete panel of all the cytokines measured is shown in Table S1. To determine whether ENaC plays a role in activation of DCs leading to cytokine production, we co-incubated the DCs with amiloride during salt exposure. We found that amiloride completely prevented the high-salt-induced production of IL-1 $\beta$  (Figure 4D). These data collectively indicate that exposure to high salt induces the formation of IsoLGs in both DCs and macrophages and causes activation of these cells.

To determine whether IsoLG-adducted peptides are presented in the major histocompatibility complexes (MHCs) of high-salt-exposed DCs, we eluted peptides from the surface of DCs treated with normal salt or high salt and performed dot blots using the D-11 antibody as shown in Figure 4E. While there was no significant difference in the total amount of peptides eluted from normal and high-salt-treated DCs (Figure 4F), the peptides obtained from high-salt-treated DCs were IsoLG adducted (Figure 4G), suggesting that salt-activated DCs process and present IsoLG-adducted peptides to T cells in their MHCs. In additional experiments, using flow cytometry and intracellular staining with the D11 antibody, we found that the high-salt-induced accumulation of IsoLGs in DCs in completely prevented by co-treatment with amiloride (Figures 4H–4J).

### **Exposure of DCs to High Salt Induces Pro-hypertensive Cytokine Production in Primed T Cells**

To verify that DCs exposed to high salt had acquired the ability to activate and induce cytokine production among T cells, we first cultured them in normal or high-salt media. We then co-cultured these cells for 3 days with T cells isolated from mice in which salt-sensitive hypertension had been induced as previously described (Itani et al., 2016) (Figure 5A). Flow cytometry was performed to identify the CD4<sup>+</sup> and CD8<sup>+</sup> T cells subsets (Figure 5B). We used fluorescence minus one (FMO) gating controls (Figures 5C, 5E, 5G, and 5I, top panels) to determine intracellular staining for interferon (IFN)- $\gamma$  and IL-17A production among the CD8<sup>+</sup> and CD4<sup>+</sup> T cells in response to DCs exposed to normal salt (Figures 5C, 5E, 5G, and 5I, middle panels) and high salt (Figures 5C, 5E, 5G, and 5I, bottom panels). As evident in Figures 5D, 5F, 5G, and 5J, DCs exposed to high salt were potent stimulators of IFN- $\gamma$  and IL-17 production among both CD8<sup>+</sup> and CD4<sup>+</sup> T cells. However, DCs exposed to high salt were not able to stimulate IFN- $\gamma$  and IL-17 production from T cells that had not been primed with salt-sensitive hypertension (Figure S1).

### **Salt-Activated DCs Sensitize Mice to a Normally Suppressor Dose of Angiotensin II, Leading to Hypertension**

To determine whether salt-activated DCs can drive hypertension, mouse splenic DCs were isolated and cultured for 24 hr in normal salt, high salt, or high salt plus the IsoLG scavenger 2-HOBA. These cells were then adoptively transferred into naive mice ( $1 \times 10^6$  DCs per mouse) via intravenous injection. Radiotelemeters were implanted to measure blood pressure and heart rate. Two weeks later, osmotic mini-pumps were implanted subcutaneously to deliver a low dose of angiotensin II (140 mg/kg/hr). This experimental

design is illustrated in Figure 6A. We found that the low dose of angiotensin II caused no increase in blood pressure in mice that received adoptive transfer of normal-salt-treated DCs; however, low-dose angiotensin II caused a significant increase in systolic (Figure 6B), diastolic (Figure 6C) and mean arterial pressure (Figure 6D), without affecting the heart rate (Figure 6E) in mice that received adoptive transfer of DCs exposed to high salt. The prohypertensive effect of high salt on DCs was prevented by scavenging of IsoLGs during the 24-hr culture (Figures 6B and 6C). These results suggest that high-salt-activated DCs prime mice to hypertension, and this is dependent on the formation of IsoLGs.

## DISCUSSION

The current studies have identified a novel pathway by which excess sodium contributes to inflammation and hypertension. Our results indicate that sodium entry into DCs is mediated through an amiloride-inhibitable sodium channel leading to intracellular calcium influx via the sodium-calcium exchanger and activation of PKC. PKC phosphorylates p47<sup>phox</sup> leading to assembly of the NADPH oxidase enzyme, increased superoxide production and immunogenic IsoLG formation in DCs. High-salt-treated DCs are activated as they have increased expression of the B7 ligand CD86 and production of the inflammatory cytokine IL-1 $\beta$ . When co-cultured with T cells, these DCs induce T cell production of pro-hypertensive cytokines IL-17 and IFN- $\gamma$ .

These studies are based on a new paradigm of salt balance that has emerged in recent years. In 2009, Machnik and colleagues showed that high-salt feeding of rodents increases interstitial concentrations of sodium in the skin to 190 mM without changing the plasma concentrations (Machnik et al., 2009; Titze et al., 2004). Subsequent studies using <sup>23</sup>Na MRI showed that similar concentrations are reached in the skin and skeletal muscle interstitium of humans with hypertension and during aging (Kopp et al., 2013). Moreover, a link has been established between such high-salt concentrations and inflammation. Recent studies have shown that exposure to high salt drives both T cells and macrophages toward an inflammatory phenotype (Jörg et al., 2016; Kleinewietfeld et al., 2013; Zhang et al., 2015). High-salt intake in humans is associated with increased numbers of circulating monocytes and higher levels of inflammatory cytokines in the plasma (Yi et al., 2015).

A key finding of the present study is that increased superoxide production is critical for the pro-inflammatory effects of high salt on DCs. While there are a number of possible sources of superoxide in the DC, our studies show that the high-salt-mediated superoxide production is dependent on the NADPH oxidase. The activity of NADPH oxidase is driven by assembly of the cytosolic subunits p40<sup>phox</sup>, p47<sup>phox</sup>, and p67<sup>phox</sup> with the membrane-bound subunits p22<sup>phox</sup> and gp91<sup>phox</sup>. When p47<sup>phox</sup> is phosphorylated, the cytosolic subunits assemble with membrane components to form a functional enzyme complex. Our results suggest that high salt regulates NADPH oxidase activity by stimulating phosphorylation of p47<sup>phox</sup>. Phosphorylation of p47<sup>phox</sup> is an obligatory step required for the assembly of the subunit complex in the cytoplasm and subsequent translocation to cytochrome b558 (gp91<sup>phox</sup> and p22<sup>phox</sup>) at the cell membrane. We demonstrate for the first time that high salt induces association of p47<sup>phox</sup> with gp91<sup>phox</sup>. We previously showed that hypertension is associated with increased superoxide production in DCs and with increased IsoLG-protein adduct

formation (Dixon et al., 2017; Kirabo et al., 2014). Our current findings illustrate a novel mechanism by which this process is stimulated by salt.

In the present studies, we focused on CD45<sup>+</sup>/MHC-II<sup>+</sup> cells that are CD11b<sup>+</sup>/CD11c<sup>+</sup>. These are compatible with monocyte-derived DCs. We previously showed, while several subtypes of DCs accumulate isoLG-adducts, this monocyte-derived population is most potently affected in hypertension and indeed can prime hypertension following adoptive transfer (Kirabo et al., 2014). In the present study, we also show salt stimulates isoLG formation in splenic macrophages, which are a related cell type.

Importantly, we found that DCs express mRNA for a number of sodium channels including the sodium-potassium 2-chloride cotransporter (NKCC2), the sodium hydrogen exchangers NHE1 and NHE6, the NCC, the sodium-calcium exchangers (NCX1 and NCX2), and the epithelial sodium channel (ENaC,  $\alpha$  and  $\gamma$  subunits). Inhibition of ENaC, NHE and NCX prevented the high-salt-induced activation of the NADPH oxidase. Amiloride and other ENaC inhibiting agents have been used clinically as diuretics for years. Our results suggest that these agents may have previously unidentified effects of inhibiting DC activation and ameliorating inflammation and have benefits beyond their natriuretic effects.

Interestingly, we found that DCs express only two subunits of ENaC (the  $\alpha$  and  $\gamma$  subunits but not the  $\beta$  subunit). ENaC is normally expressed in the apical membrane of polarized epithelial cells including the distal nephron, colon, and the airway epithelium. Its function is best characterized in the distal nephron where it serves as the rate-limiting step for reabsorption of sodium under the control of aldosterone and vasopressin. Activating mutations of ENaC cause severe disturbances of Na<sup>+</sup> homeostasis leading to hypertension in humans and in mouse models. In the kidney, ENaC is composed of three subunits including the  $\alpha$ ,  $\beta$ , and  $\gamma$  subunits. Although all these subunits are required to give maximal channel activity, several studies have demonstrated that in *Xenopus* oocytes,  $\alpha_2\gamma_2$  heterotetramers conduct 10%–15% of the activity observed with all three subunits (Bonny et al., 1999; Chang et al., 1996; Loffing et al., 2001; Rubera et al., 2003).

NCX can function in a forward mode, exchanging extracellular Na<sup>+</sup> for intracellular Ca<sup>2+</sup>, or in reverse mode, depending on the Na<sup>+</sup> and Ca<sup>2+</sup> gradients across plasma membrane (Annunziato et al., 2004). Under physiological conditions, the main function of NCX is to extrude Ca<sup>2+</sup> from cells. However, in pathophysiological conditions such as ischemia and early reperfusion, the higher intracellular Na<sup>+</sup> concentrations can cause the NCX to function in reverse mode coupling Ca<sup>2+</sup> influx with Na<sup>+</sup> efflux (Imahashi et al., 2005; Kusuoka et al., 1993; Mattiello et al., 1998). In the present studies, we found that sodium entry into DCs is achieved through ENaC and NHE leading to increased intracellular Na<sup>+</sup>. This resulted in an initial brief reduction, followed by a subsequent influx of intracellular Ca<sup>2+</sup> (Figures 2E and 2F), suggesting that, in the context of high-salt exposure, NCX in DCs switches from operating in forward mode to operating in the reverse mode. Indeed, our results suggest that the salt-mediated activation of the NADPH-oxidase is dependent on this intracellular Ca<sup>2+</sup> influx as it was prevented by the cell permeant Ca<sup>2+</sup>-specific chelator, BAPTA, AM. The upstream pathways leading to activation of the NADPH oxidase vary considerably. One such pathway is phosphorylation of p47<sup>phox</sup> by Ca<sup>2+</sup>-dependent PKC isoforms. In keeping with

this, the high-salt-induced activation of the NADPH oxidase was completely abolished by PKC inhibition with calphostin C (20 nM, Figure 2D).

A notable finding is that salt promoted production of IL-1 $\beta$  by DCs. This is in keeping with prior observations made by Shapiro and Dinarello, who showed that increased salt drives production of this cytokine by peripheral blood mononuclear cells (Shapiro and Dinarello, 1997). Interestingly, Zhang et al. recently showed that IL-1 $\beta$  receptor blockade blunts hypertension and salt retention by effects on NKCC2 in the nephron (Zhang et al., 2016). IL-1 $\beta$  contributes to priming T cells for production of IL-17A, which mediates hypertension and end-organ dysfunction (Madhur et al., 2010; Nguyen et al., 2013).

In conclusion, we have identified a previously unknown role of excess extracellular sodium in activating antigen-presenting DCs via formation of IsoLGs, which, in turn, promote hypertension. These findings provide insight into how elevated sodium microenvironments, such as those found in the interstitium of hypertensive animals and humans can lead to an inflammatory state and hypertension. Drugs that inhibit sodium entry into DCs may have previously unknown antioxidant and anti-inflammatory properties.

## EXPERIMENTAL PROCEDURES

### Animals

Wild-type C57BL/6 mice were obtained from Jackson Laboratories. All experiments were performed in male animals at approximately 3 months of age. Osmotic mini-pumps (Alzet, Model 2002) were implanted for infusion of low-dose angiotensin II (140 ng/kg/min) for 2 weeks. Blood pressure was monitored invasively using radio-telemetry as previously described (Guzik et al., 2007; Kirabo et al., 2011a, 2011b). After telemetry implantation, mice were allowed to recover for 10 days before osmotic mini-pumps were placed. Adoptive transfer of DCs was accomplished by injection  $1 \times 10^6$  DCs in 100  $\mu$ L of sterile physiological buffered saline via the retro-orbital vein in mice anesthetized with 2% isoflurane. Angiotensin II infusion was started 10 days after adoptive transfer of DCs. The L-NAME high-salt protocol was performed as previously described (Itani et al., 2016). Briefly, at 12 weeks of age, male mice were randomly selected to initially receive L-NAME (0.5 mg/mL, Abcam 120136) in the drinking water for 2 weeks. This was followed by a 2-week washout period when the mice were given regular water and chow ad libitum. The mice were then fed a high-salt diet (4% NaCl, Teklad TD.92034) for 3 weeks. Mice were sacrificed at the end of all experiments by CO<sub>2</sub> inhalation. All animal procedures were approved by Vanderbilt University's Institutional Animal Care and Use Committee, and the mice were housed and cared for in accordance with the Guide for the Care and Use of Laboratory Animals, US Department of Health and Human Services.

### Splenocyte and DC Isolation and Culture

Mouse splenic DCs were isolated using magnetic-activated cell sorting (MACS). Mice were euthanized with CO<sub>2</sub>, and spleens were removed and placed in spleen dissociation buffer in C tubes (Miltenyi). Spleens were dissociated using homogenizer (Miltenyi) and incubated at 37°C for 15 min. Homogenate was then passed through a 40- $\mu$ m cell strainer and washed

with Dulbecco's PBS (dPBS). For splenocyte experiments, this single-cell suspension was then cultured for 24 hr in either control RPMI media (150 mmol/L Na<sup>+</sup>) or media containing 190 mmol/L Na<sup>+</sup>. To control for hyperosmolality, other cells were exposed to mannitol (190 mmol/L). For DC-specific experiments, DCs were then isolated from this single-cell suspension using the CD11c isolation kit (Miltenyi). For T cell activation experiments, DCs were cultured with T cells (Pan T Cell Isolation Kit II, mouse, 130-095-130) isolated from mice with repeated hypertensive stimuli challenges for 3 days.

### Flow Cytometry

DCs were analyzed by flow cytometry using the following antibodies; PerCP-Cy5.5 anti-CD45; Amcyan anti-CD45; PE-Cy7 anti-I-Ab; PerCP-Cy5.5 anti-CD11c; APC-Cy7 anti-CD11b; PE anti MertK, and APC anti CD64 (Becton Dickinson). We used intracellular staining with the single-chain antibody D-11 to detect IsoLG protein adducts. D-11 is a single-chain antibody that was developed by phage display screening of literally millions of single chains to identify one that reacts with isoLGs adducted to any peptide backbone (Davies et al., 2004). The D11 ScFv antibody was labeled with a fluorochrome using the APEXTM Alexa Fluor 488 Antibody Labeling kit (Invitrogen). The cells labeled with surface antibodies were then fixed and permeabilized for intracellular detection of IsoLGs using a cell permeabilization kit (Invitrogen). For T cell analysis, the following antibodies were used: Brilliant Violet 510 (BV510)-conjugated anti-CD45 antibody (BioLegend), peridinin chlorophyll protein-cyanin-5.5 (PerCP-Cy5.5)-conjugated anti-CD3 antibody (BioLegend), phycoerythrin-cyanin-7(PE-Cy7)-conjugated anti-CD8 antibody (BioLegend), and allophycocyanin-Hilite-7 (APC-H7)-conjugated anti-CD4 antibody (BD Biosciences). Intracellular staining for IL-17A and IFN- $\gamma$  were performed as previously described (Itani et al., 2016; Kamat et al., 2015). Briefly, T cells were suspended in RPMI medium supplemented with 5% FBS and stimulated with 2  $\mu$ L of BD Leukocyte Activation Cocktail (ionomycin and phorbol myristic acetate (PMA) along with the Golgi inhibitor, brefeldin A) at 37°C for 5 hr. Surface staining was performed as described above followed by intracellular staining using fluorescein isothiocyanate (FITC)-conjugated anti-IFN- $\gamma$  antibody (eBioscience) or PE-conjugated anti-IL-17A. The cells were then washed 3 times and immediately analyzed on a FACSCanto flow cytometer with DIVA software (Becton Dickinson). Dead cells were eliminated from the analysis using 7-AAD (BD Pharmingen). For each experiment, we gated on single live cells and used flow minus one (FMO) controls for each fluorophore to establish the gates. Data analysis was done using FlowJo software (Tree Star).

### Weak Acid Elution of DC MHC-Associated Peptides

DCs were placed in citrate-phosphate buffer at pH 3.3 containing aprotinin and iodoacetamide (1:100) to elute MHC-I-bound peptides. The peptides were then be passed through ultrafiltration devices (Amicon Ultra; Millipore) to isolate peptides <5,000 Da and to remove beta-2 microglobulin ( $\beta$ 2 m) proteins. The concentration of the peptides in the resulting flow-through was determined using a nanodrop and analyzed by dot blot using the D-11 antibody.

### ESR Measurements of Superoxide Production in DCs

DCs were isolated from the spleen of C57BL/6 mice and placed in the RPMI cell-culture media in the presence of normal (140 mM) or high NaCl (190 mM) for 24 hr. Cells were placed in 24-well plate with 2 million cells per well. Some cells were supplemented with peptide gp91 ds-tat (50  $\mu$ M, GenScript) which inhibits assembly of the NADPH oxidase enzyme. After 24 hr, cells were resuspended and treated spin probe TMH (0.5 mM) and chelating agent DTPA (0.1 mM) as we have previously described (Dikalov et al., 2011). Following 30-min incubation, cells were transferred in a 1-mL insulin syringe and snap-frozen in the liquid nitrogen. Then frozen cells were placed in the quartz Dewar with the liquid nitrogen and analyzed by Bruker EMX ESR spectrometer. Accumulation of superoxide-TMH nitroxide product was determined from the intensity of ESR signal using standard calibration obtained with TEMPOL nitroxide. Superoxide specificity of ESR signal was confirmed by inhibition with the NADPH oxidase inhibitor peptide gp91 ds-tat (Dikalov et al., 2014).

### Real-Time RT-PCR

The total RNA was extracted using QIAzolLysis Reagent (QIAGEN) according to manufacturer's instructions. The concentration and purity of the isolated RNA were determined using UV spectrophotometry (DeNovix Spectrophotometer). Reverse transcription was performed using TaqMan Reverse Transcription Reagents (Life Technologies) using 1  $\mu$ g of total RNA. Real-time RT-PCR was performed using TaqMan Gene Expression Assays. Gene expression values were calculated based on the comparative Ct normalized to the expression values of GAPDH mRNA and displayed as fold induction. The PCR parameters were: an initial denaturation (one cycle at 95°C for 10 min); denaturation at 95°C for 10 s, annealing and amplification at 60°C for 30 s for 40 cycles; and a melting curve, 72°C, with the temperature gradually increasing (0.5°C) to 95°C.

### Intracellular Sodium Measurements

Intracellular Na<sup>+</sup> was measured with the sodium-sensitive fluorescent probe, sodium green (Molecular Probes), using flow cytometry as described previously (Sugishita et al., 2001). Briefly, cells were loaded with 5  $\mu$ mol/L sodium green AM in HEPES solution for 60 min at 37°C. Loaded cells were then washed and incubated in dye-free HEPES solution for 10 min. The cells were separated into aliquots and exposed to either normal (150 mM NaCl) or high salt (190 mM NaCl) for 15 min. The cells were then immediately analyzed by flow cytometry on a FACSCanto flow cytometer with DIVA software (Becton Dickinson). Dead cells were eliminated from the analysis using 7-AAD (BD Pharmingen). Cells that were not loaded with the sodium green fluorescent probe were used as controls to establish the gates. Data analysis was done using FlowJo software (Tree Star).

### Immunoblotting

Immunoprecipitation and western blot analysis were performed as previously described (Sayeski et al., 1998). To determine phosphorylation of p47<sup>phox</sup>, protein sample was extracted from the homogenates of isolated DCs and immunoprecipitated using p47<sup>phox</sup> antibody (Millipore) followed by western blotting using phospho-p47<sup>phox</sup> antibody (Sigma).

To investigate association of p47<sup>phox</sup> with gp91<sup>phox</sup>, protein lysates from DCs were immunoprecipitated using the gp91<sup>phox</sup> antibody (Becton Dickinson) followed by western blotting using phospho-p47<sup>phox</sup> antibody (Millipore).

### Ca<sup>2+</sup> Fluorescence Measurements

DCs were isolated as described above and rested overnight in RPMI media. The cells were then loaded with membrane-permeable Ca<sup>2+</sup>-sensitive fluorescent indicator Fluo-4 AM. Cells were incubated in Tyrode's solution (in mM: NaCl 140, KCl 5.4, MgCl<sub>2</sub> 1, glucose 10, HEPES 10), containing 1 mM Ca<sup>2+</sup>, 6.6 μM fluo-4 AM, and 0.16% Pluronic F127 for 20 min at room temperature to load indicator in the cytosol. Then the supernatant was removed, and cells were washed in Tyrode's solution, containing 1 mM Ca<sup>2+</sup>, twice for 15 min. After that, the cells were placed into the experimental chamber superfused with 2 mM Ca<sup>2+</sup> Tyrode's solution. Intracellular Ca<sup>2+</sup> was measured using fluorescence photometry setup (IonOptix). Ca<sup>2+</sup> fluorescence was first measured after 3–5 min in normal salt (140 mmol/L Na<sup>+</sup>), and then solution was changed to high salt (190 mmol/L Na) and Ca<sup>2+</sup> fluorescence was monitored in 3-min intervals for another 21–24 min. All experiments were conducted at room temperature (≈23°C). Intracellular Ca<sup>2+</sup> was analyzed using commercial software (IonWizard; IonOptix). A total of 7–12 DCs from nine different animals were used.

### siRNA Experiments

Mouse splenic DCs were isolated using MACS. Four million cells were re-suspended in 1 mL of Accell siRNA delivery medium (GE Healthcare Dharmacon) supplemented with 2.5% FBS, 1 mM sodium pyruvate and 25 mM HEPES. Cells were incubated for 72 hr with 1 μM Accell SMART pool of siRNA targeting mouse NHE1 (*Slc9a1* siRNA [E-048336-00-0005], or Alpha ENaC (*Scnn1a* [E-040678-00-0005] GE Healthcare Dharmacon). ON-TARGETplus Non-targeting Control siRNA (D-001810-01-05) was used as a negative control. Sodium chloride (40 mM) was added for additional 24 hr. The knockdown levels of Alpha ENaC and NHE1 were analyzed by western blot.

### Inhibitors

Furosemide (20 μM Tocris Bioscience), hydrochlorothiazide (20 μM, Sigma), amiloride (20 μM, Tocris Bioscience), benzamil hydrochloride hydrate (10 μM, Sigma), KB-R7943 mesylate (2 nM, Tocris Bioscience), 1,2-bis(o-aminophenoxy) ethane-N,N,N',N'-tetraacetic acid (BAPTA, AM) (Tocris Bioscience), calphostin C (20 nM, Sigma), cariporide (10 μM, Sigma), and nickel chloride (NiCl<sub>2</sub>) (10 mM, Sigma).

### Statistical Analysis

All data are expressed as mean ± SEM. Comparisons made between 2 variables were performed using Student's t tests. One-way ANOVA was used to compare 3 or more independent groups with post hoc analysis Tukey's post hoc test, while repeated-measures ANOVA was used to compare changes in blood pressure over time. The level of significance (α) accepted was less than 0.05.

## Supplementary Material

Refer to Web version on PubMed Central for supplementary material.

## Acknowledgments

This work was supported by American Heart Association grants POST290900 and SFRN204200, National Institutes of Health grants K01HL130497, R01HL125865, and R01HL039006, and the National Center for Advancing Translational Sciences (UL1TR000445). We thank Kala B. Dixon and Anica Mohammadkhah for the technical help with experiments.

## References

- Annunziato L, Pignataro G, Di Renzo GF. Pharmacology of brain Na<sup>+</sup>/Ca<sup>2+</sup> exchanger: From molecular biology to therapeutic perspectives. *Pharmacol. Rev.* 2004; 56:633–654. [PubMed: 15602012]
- Benjamin EJ, Blaha MJ, Chiuve SE, Cushman M, Das SR, Deo R, de Ferranti SD, Floyd J, Fornage M, Gillespie C, et al. American Heart Association Statistics, C.; Stroke Statistics, S. Heart disease and stroke statistics-2017 update: a report from the American Heart Association. *Circulation.* 2017; 135:e146–e603. [PubMed: 28122885]
- Binger KJ, Gebhardt M, Heinig M, Rintisch C, Schroeder A, Neuhofer W, Hilgers K, Manzel A, Schwartz C, Kleinewietfeld M, et al. High salt reduces the activation of IL-4- and IL-13-stimulated macrophages. *J. Clin. Invest.* 2015; 125:4223–4238. [PubMed: 26485286]
- Bonny O, Chraïbi A, Loffing J, Jaeger NF, Gründer S, Horisberger JD, Rossier BC. Functional expression of a pseudohypoaldosteronism type I mutated epithelial Na<sup>+</sup> channel lacking the pore-forming region of its alpha subunit. *J. Clin. Invest.* 1999; 104:967–974. [PubMed: 10510337]
- Chang SS, Grunder S, Hanukoglu A, Rösler A, Mathew PM, Hanukoglu I, Schild L, Lu Y, Shimkets RA, Nelson-Williams C, et al. Mutations in subunits of the epithelial sodium channel cause salt wasting with hyperkalaemic acidosis, pseudohypoaldosteronism type 1. *Nat. Genet.* 1996; 12:248–253. [PubMed: 8589714]
- Chiasson VL, Talreja D, Young KJ, Chatterjee P, Banes-Berceli AK, Mitchell BM. FK506 binding protein 12 deficiency in endothelial and hematopoietic cells decreases regulatory T cells and causes hypertension. *Hypertension.* 2011; 57:1167–1175. [PubMed: 21518963]
- Davies SS, Talati M, Wang X, Mernaugh RL, Amarnath V, Fessel J, Meyrick BO, Sheller J, Roberts LJ 2nd. Localization of isoketal adducts in vivo using a single-chain antibody. *Free Radic. Biol. Med.* 2004; 36:1163–1174. [PubMed: 15082070]
- Dikalov SI, Kirilyuk IA, Voinov M, Grigor'ev IA. EPR detection of cellular and mitochondrial superoxide using cyclic hydroxylamines. *Free Radic. Res.* 2011; 45:417–430. [PubMed: 21128732]
- Dikalov SI, Nazarewicz RR, Bikineyeva A, Hilenski L, Lassegue B, Griendling KK, Harrison DG, Dikalova AE. Nox2-induced production of mitochondrial superoxide in angiotensin II-mediated endothelial oxidative stress and hypertension. *Antioxid. Redox. Signal.* 2014; 20:281–294. [PubMed: 24053613]
- Dixon KB, Davies SS, Kirabo A. Dendritic cells and isolevuglandins in immunity, inflammation and hypertension. *Am. J. Physiol. Heart Circ. Physiol.* 2017; 312:H368–H374. [PubMed: 27986660]
- Garcia RC, Whitaker M, Heyworth PG, Segal AW. Okadaic acid produces changes in phosphorylation and translocation of proteins and in intracellular calcium in human neutrophils. Relationship with the activation of the NADPH oxidase by different stimuli. *Biochem. J.* 1992; 286:687–692. [PubMed: 1417726]
- Guzik TJ, Hoch NE, Brown KA, McCann LA, Rahman A, Dikalov S, Goronzy J, Weyand C, Harrison DG. Role of the T cell in the genesis of angiotensin II induced hypertension and vascular dysfunction. *J. Exp. Med.* 2007; 204:2449–2460. [PubMed: 17875676]
- Ha SK. Dietary salt intake and hypertension. *Electrolyte Blood Press.* 2014; 12:7–18. [PubMed: 25061468]

- Imahashi K, Pott C, Goldhaber JJ, Steenbergen C, Philipson KD, Murphy E. Cardiac-specific ablation of the Na<sup>+</sup>-Ca<sup>2+</sup> exchanger confers protection against ischemia/reperfusion injury. *Circ. Res.* 2005; 97:916–921. [PubMed: 16179590]
- Itani HA, Xiao L, Saleh MA, Wu J, Pilkinton MA, Dale BL, Barbaro NR, Foss JD, Kirabo A, Montaniel KR, et al. CD70 exacerbates blood pressure elevation and renal damage in response to repeated hypertensive stimuli. *Circ. Res.* 2016; 118:1233–1243. [PubMed: 26988069]
- Jakubzick C, Gautier EL, Gibbings SL, Sojka DK, Schlitzer A, Johnson TE, Ivanov S, Duan Q, Bala S, Condon T, et al. Minimal differentiation of classical monocytes as they survey steady-state tissues and transport antigen to lymph nodes. *Immunity.* 2013; 39:599–610. [PubMed: 24012416]
- Jantsch J, Schatz V, Friedrich D, Schröder A, Kopp C, Siegert I, Maronna A, Wendelborn D, Linz P, Binger KJ, et al. Cutaneous Na<sup>+</sup> storage strengthens the antimicrobial barrier function of the skin and boosts macrophage-driven host defense. *Cell Metab.* 2015; 21:493–501. [PubMed: 25738463]
- Jörg S, Kissel J, Manzel A, Kleinewietfeld M, Haghikia A, Gold R, Müller DN, Linker RA. High salt drives Th17 responses in experimental autoimmune encephalomyelitis without impacting myeloid dendritic cells. *Exp. Neurol.* 2016; 279:212–222. [PubMed: 26976739]
- Kamat NV, Thabet SR, Xiao L, Saleh MA, Kirabo A, Madhur MS, Delpire E, Harrison DG, McDonough AA. Renal transporter activation during angiotensin-II hypertension is blunted in interferon- $\gamma$ <sup>-/-</sup> and interleukin-17A<sup>-/-</sup> mice. *Hypertension.* 2015; 65:569–576. [PubMed: 25601932]
- Kearney PM, Whelton M, Reynolds K, Muntner P, Whelton PK, He J. Global burden of hypertension: Analysis of worldwide data. *Lancet.* 2005; 365:217–223. [PubMed: 15652604]
- Kirabo A, Kearns PN, Jarajapu YP, Sasser JM, Oh SP, Grant MB, Kasahara H, Cardounel AJ, Baylis C, Wagner KU, Sayeski PP. Vascular smooth muscle Jak2 mediates angiotensin II-induced hypertension via increased levels of reactive oxygen species. *Cardiovasc. Res.* 2011a; 91:171–179. [PubMed: 21354995]
- Kirabo A, Oh SP, Kasahara H, Wagner KU, Sayeski PP. Vascular smooth muscle Jak2 deletion prevents angiotensin II-mediated neo-intima formation following injury in mice. *J. Mol. Cell. Cardiol.* 2011b; 50:1026–1034. [PubMed: 21420414]
- Kirabo A, Fontana V, de Faria AP, Loperena R, Galindo CL, Wu J, Bikineyeva AT, Dikalov S, Xiao L, Chen W, et al. DC isoketal-modified proteins activate T cells and promote hypertension. *J. Clin. Invest.* 2014; 124:4642–4656. [PubMed: 25244096]
- Kleinewietfeld M, Manzel A, Titze J, Kvakana H, Yosef N, Linker RA, Müller DN, Hafler DA. Sodium chloride drives autoimmune disease by the induction of pathogenic TH17 cells. *Nature.* 2013; 496:518–522. [PubMed: 23467095]
- Kopp C, Linz P, Dahlmann A, Hammon M, Jantsch J, Müller DN, Schmieder RE, Cavallaro A, Eckardt KU, Uder M, et al. <sup>23</sup>Na magnetic resonance imaging-determined tissue sodium in healthy subjects and hypertensive patients. *Hypertension.* 2013; 61:635–640. [PubMed: 23339169]
- Kusuoka H, Camilion de Hurtado MC, Marban E. Role of sodium/calcium exchange in the mechanism of myocardial stunning: Protective effect of reperfusion with high sodium solution. *J. Am. Coll. Cardiol.* 1993; 21:240–248. [PubMed: 8417067]
- Loffing J, Zecevic M, Féraillé E, Kaissling B, Asher C, Rossier BC, Firestone GL, Pearce D, Verrey F. Aldosterone induces rapid apical translocation of ENaC in early portion of renal collecting system: Possible role of SGK. *Am. J. Physiol. Renal Physiol.* 2001; 280:F675–F682. [PubMed: 11249859]
- Machnik A, Neuhofer W, Jantsch J, Dahlmann A, Tammela T, Machura K, Park JK, Beck FX, Müller DN, Derer W, et al. Macrophages regulate salt-dependent volume and blood pressure by a vascular endothelial growth factor-C-dependent buffering mechanism. *Nat. Med.* 2009; 15:545–552. [PubMed: 19412173]
- Madhur MS, Lob HE, McCann LA, Iwakura Y, Blinder Y, Guzik TJ, Harrison DG. Interleukin 17 promotes angiotensin II-induced hypertension and vascular dysfunction. *Hypertension.* 2010; 55:500–507. [PubMed: 20038749]
- Mattiello JA, Margulies KB, Jeevanandam V, Houser SR. Contribution of reverse-mode sodium-calcium exchange to contractions in failing human left ventricular myocytes. *Cardiovasc. Res.* 1998; 37:424–431. [PubMed: 9614497]

- Mattson DL, Lund H, Guo C, Rudemiller N, Geurts AM, Jacob H. Genetic mutation of recombination activating gene 1 in Dahl salt-sensitive rats attenuates hypertension and renal damage. *Am. J. Physiol. Regul. Integr. Comp. Physiol.* 2013; 304:R407–R414. [PubMed: 23364523]
- McMaster WG, Kirabo A, Madhur MS, Harrison DG. Inflammation, immunity, and hypertensive end-organ damage. *Circ. Res.* 2015; 116:1022–1033. [PubMed: 25767287]
- Mills KH. Induction, function and regulation of IL-17-producing T cells. *Eur. J. Immunol.* 2008; 38:2636–2649. [PubMed: 18958872]
- Murray CJ, Lopez AD. Measuring the global burden of disease. *N. Engl. J. Med.* 2013; 369:448–457. [PubMed: 23902484]
- Nguyen H, Chiasson VL, Chatterjee P, Kopriva SE, Young KJ, Mitchell BM. Interleukin-17 causes Rho-kinase-mediated endothelial dysfunction and hypertension. *Cardiovasc. Res.* 2013; 97:696–704. [PubMed: 23263331]
- Papini E, Grzeskowiak M, Bellavite P, Rossi F. Protein kinase C phosphorylates a component of NADPH oxidase of neutrophils. *FEBS Lett.* 1985; 190:204–208. [PubMed: 4043401]
- Rubera I, Loffing J, Palmer LG, Frindt G, Fowler-Jaeger N, Sauter D, Carroll T, McMahon A, Hummler E, Rossier BC. Collecting duct-specific gene inactivation of alphaENaC in the mouse kidney does not impair sodium and potassium balance. *J. Clin. Invest.* 2003; 112:554–565. [PubMed: 12925696]
- Sayeski PP, Ali MS, Harp JB, Marrero MB, Bernstein KE. Phosphorylation of p130Cas by angiotensin II is dependent on c-Src, intracellular Ca<sup>2+</sup>, and protein kinase. *C. Circ. Res.* 1998; 82:1279–1288. [PubMed: 9648724]
- Shapiro L, Dinarello CA. Hyperosmotic stress as a stimulant for proinflammatory cytokine production. *Exp. Cell Res.* 1997; 231:354–362. [PubMed: 9087177]
- Sugishita K, Su Z, Li F, Philipson KD, Barry WH. Gender influences [Ca(2+)]<sub>i</sub> during metabolic inhibition in myocytes overexpressing the Na(+)-Ca(2+) exchanger. *Circulation.* 2001; 104:2101–2106. [PubMed: 11673353]
- Titze J, Machnik A. Sodium sensing in the interstitium and relationship to hypertension. *Curr. Opin. Nephrol. Hypertens.* 2010; 19:385–392. [PubMed: 20571401]
- Titze J, Shakibaei M, Schafflhuber M, Schulze-Tanzil G, Porst M, Schwind KH, Dietsch P, Hilgers KF. Glycosaminoglycan polymerization may enable osmotically inactive Na<sup>+</sup> storage in the skin. *Am. J. Physiol. Heart Circ. Physiol.* 2004; 287:H203–H208. [PubMed: 14975935]
- Vinh A, Chen W, Blinder Y, Weiss D, Taylor WR, Goronzy JJ, Weyand CM, Harrison DG, Guzik TJ. Inhibition and genetic ablation of the B7/CD28 T-cell costimulation axis prevents experimental hypertension. *Circulation.* 2010; 122:2529–2537. [PubMed: 21126972]
- Wu C, Yosef N, Thalhamer T, Zhu C, Xiao S, Kishi Y, Regev A, Kuchroo VK. Induction of pathogenic TH17 cells by inducible salt-sensing kinase SGK1. *Nature.* 2013; 496:513–517. [PubMed: 23467085]
- Yi B, Titze J, Rykova M, Feuerecker M, Vassilieva G, Nichiporuk I, Schelling G, Morukov B, Choukèr A. Effects of dietary salt levels on monocytic cells and immune responses in healthy human subjects: A longitudinal study. *Transl. Res.* 2015; 166:103–110. [PubMed: 25497276]
- Youn JC, Yu HT, Lim BJ, Koh MJ, Lee J, Chang DY, Choi YS, Lee SH, Kang SM, Jang Y, Yoo OJ, Shin EC, Park S. Immunosenescent CD8<sup>+</sup> T cells and C-X-C chemokine receptor type 3 chemokines are increased in human hypertension. *Hypertension.* 2013; 62:126–133. [PubMed: 23716586]
- Zhang WC, Zheng XJ, Du LJ, Sun JY, Shen ZX, Shi C, Sun S, Zhang Z, Chen XQ, Qin M, et al. High salt primes a specific activation state of macrophages, M(Na). *Cell Res.* 2015; 25:893–910. [PubMed: 26206316]
- Zhang J, Rudemiller NP, Patel MB, Karlovich NS, Wu M, McDonough AA, Griffiths R, Sparks MA, Jeffs AD, Crowley SD. Interleukin-1 receptor activation potentiates salt reabsorption in angiotensin II-induced hypertension via the NKCC2 co-transporter in the nephron. *Cell Metab.* 2016; 23:360–368. [PubMed: 26712462]

### Highlights

- Increased extracellular sodium is transported into DCs by amiloride-sensitive channels
- Sodium is exchanged for calcium, activating  $O_2^{\cdot-}$  formation by the NADPH oxidase
- Enhanced  $O_2^{\cdot-}$  in DCs leads to formation of isolevuglandin protein adducts
- Salt-stimulated DCs produce pro-inflammatory cytokines and drive T cell activation

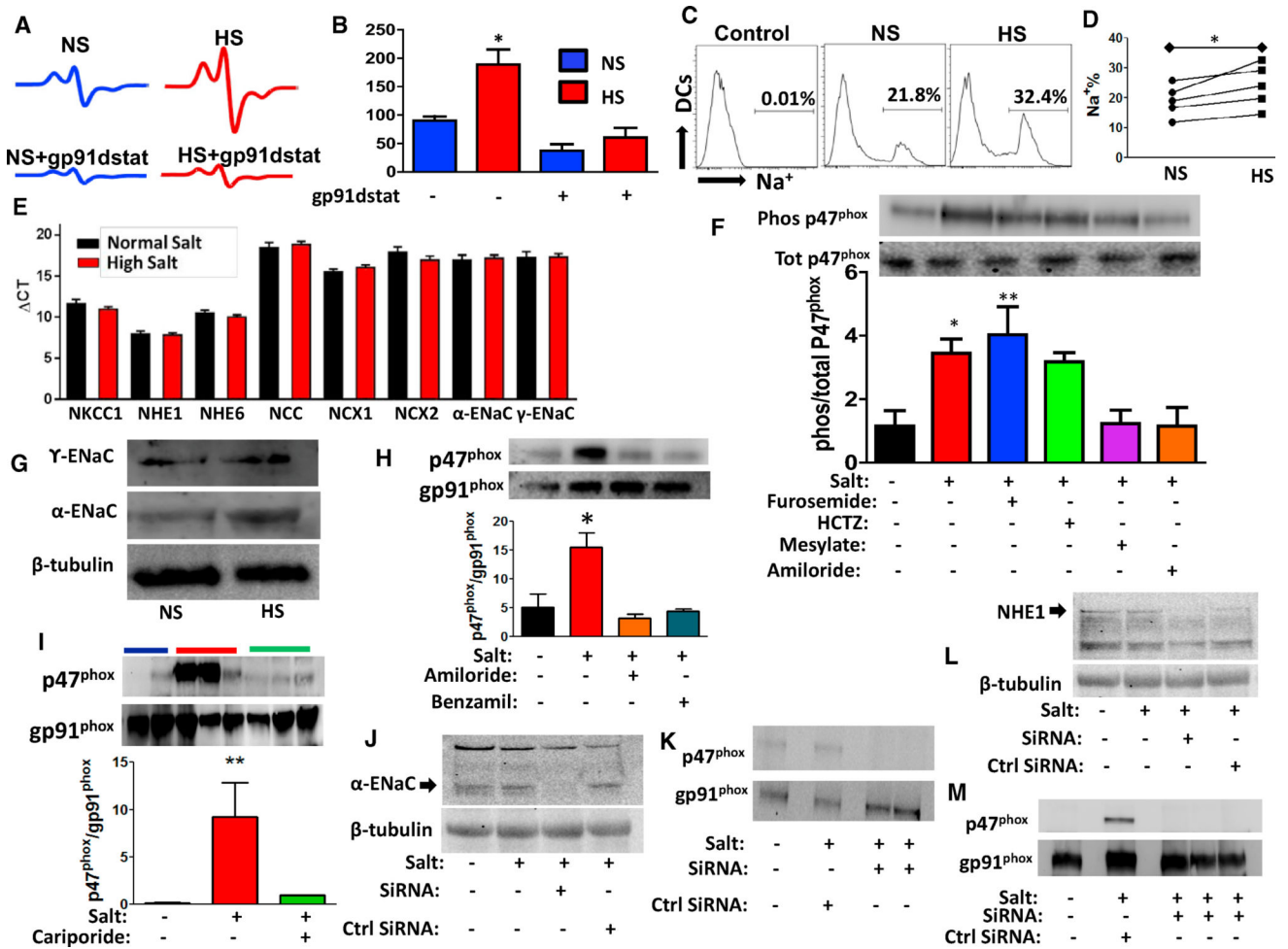


**Figure 1. High Salt Activates the NADPH Oxidase in Dendritic Cells Leading to Increased Superoxide Production through an Amiloride-Inhibitible Sodium Channel and Sodium-Calcium Exchanger**

Mouse splenic dendritic cells were isolated and cultured for 24 hr in either normal-salt (150 mM NaCl) or high-salt (190 mM NaCl) media with or without the NADPH oxidase inhibitor, gp91dstat. Superoxide production was then measured by electron spin resonance. (A) Representative ESR signals showing the effect of high salt and gp91 ds-tat on dendritic cell superoxide production. (B) Average data showing the effect of high salt and gp91 ds-tat on dendritic cell superoxide production. (C) Flow cytometry representative histograms showing the effect of 15 min high-salt exposure on intracellular sodium. (D) Average data showing the effect of high salt on intracellular sodium. (E) qRT-PCR of sodium transporters: sodium-potassium-chloride cotransporter-1 (NKCC1), the sodium hydrogen exchangers (NHE1 and NHE6), the NCC, the sodium-calcium exchangers (NCX1 and NCX2), and the epithelial sodium channel (ENaC,  $\alpha$  and  $\gamma$  subunits) on dendritic cells treated with normal or high salt. (F) Effect of sodium transporter inhibitors on phosphorylation of p47<sup>phox</sup>.

- (G) Western blot showing presence of the ENaC,  $\alpha$  and  $\gamma$  subunits in dendritic cells treated with normal or high salt.
- (H) Effect of amiloride and benzamil on the high-salt-induced association of p47<sup>phox</sup> and gp91<sup>phox</sup>.
- (I) Effect of the Na<sup>+</sup>/H<sup>+</sup> exchange inhibitor cariporide on the high-salt-induced association of p47<sup>phox</sup> and gp91<sup>phox</sup>.
- (J) Effect of  $\alpha$ -ENaC targeted siRNA and non-targeting siRNA on expression of  $\alpha$ -ENaC.
- (K) Effect of knockdown of  $\alpha$ -ENaC on association of p47<sup>phox</sup> with gp91<sup>phox</sup>.
- (L) Effect of NHE1 targeted siRNA and non-targeting siRNA on expression of NHE1.
- (M) Effect of siRNA-mediated knockdown of NHE1 on the association of p47<sup>phox</sup> with gp91<sup>phox</sup>. (n = 5–6, \*p < 0.05, \*\*p < 0.01 versus normal-salt control, expressed as mean  $\pm$  SEM).

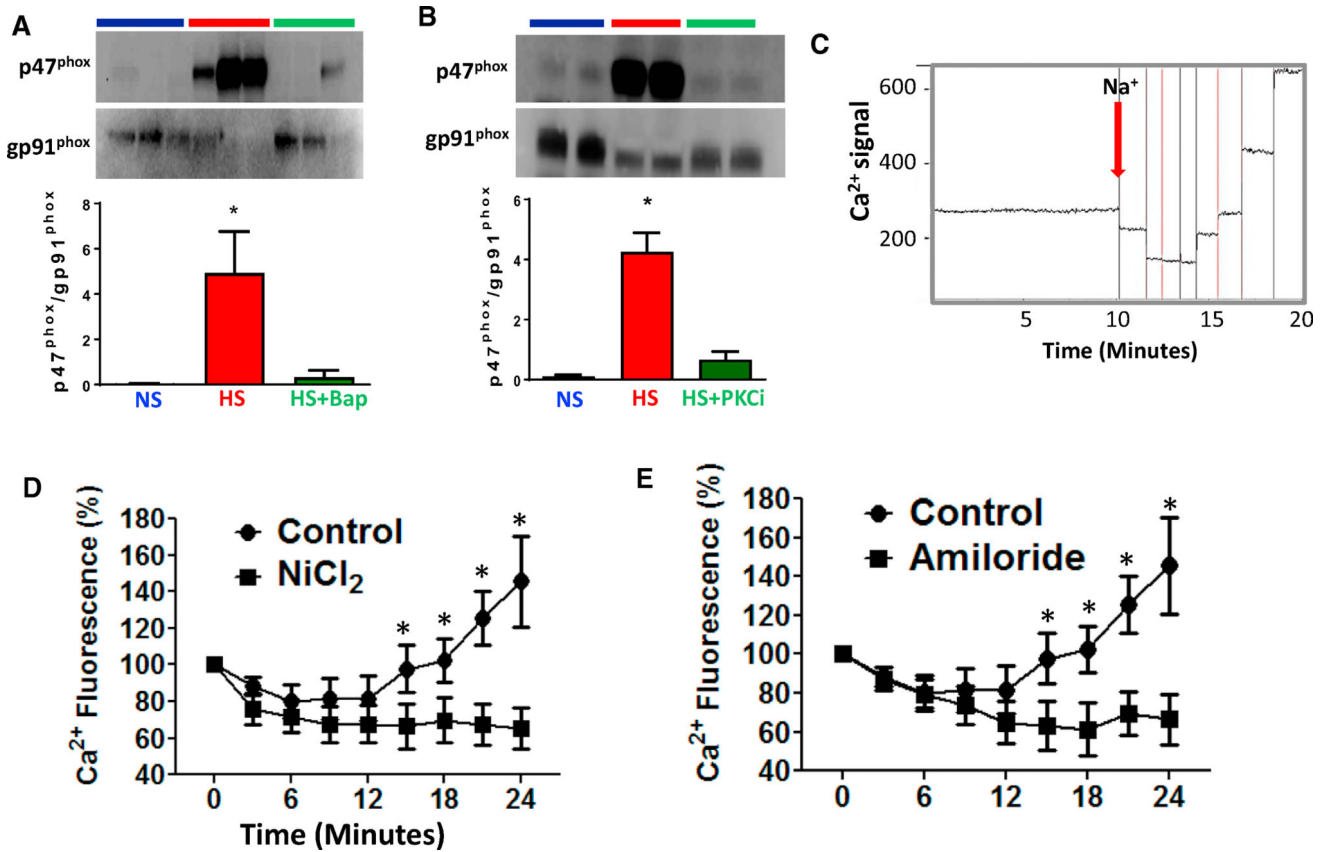


### Figure 2. Salt-Induced Activation of the NADPH Oxidase in Dendritic Cells Is Calcium- and PKC Dependent

Splenic dendritic cell lysates were immunoprecipitated for gp91<sup>phox</sup>, p47<sup>phox</sup> western blot was performed, the membranes were stripped, and gp91<sup>phox</sup> western blot was performed.

(A) Effect of BAPTA-AM on the high-salt-induced association of p47<sup>phox</sup> with gp91<sup>phox</sup>.

(B) Effect of the PKC inhibitor calphostin C on the high-salt-induced association of p47<sup>phox</sup> and gp91<sup>phox</sup>.

(C) Representative tracing showing intracellular Ca<sup>2+</sup> in a single dendritic cell in response to high salt using fluorescence photometry (IonOptix).

(D) Average data showing the effect of the sodium calcium exchanger blocker, nickel chloride, on the high-salt-induced intracellular Ca<sup>2+</sup> influx in dendritic cells.

(E) Average data showing the effect of amiloride on the high-salt-induced intracellular Ca<sup>2+</sup> influx in dendritic cells (n = 3–12, \*p < 0.05 versus normal-salt control, expressed as mean ± SEM).

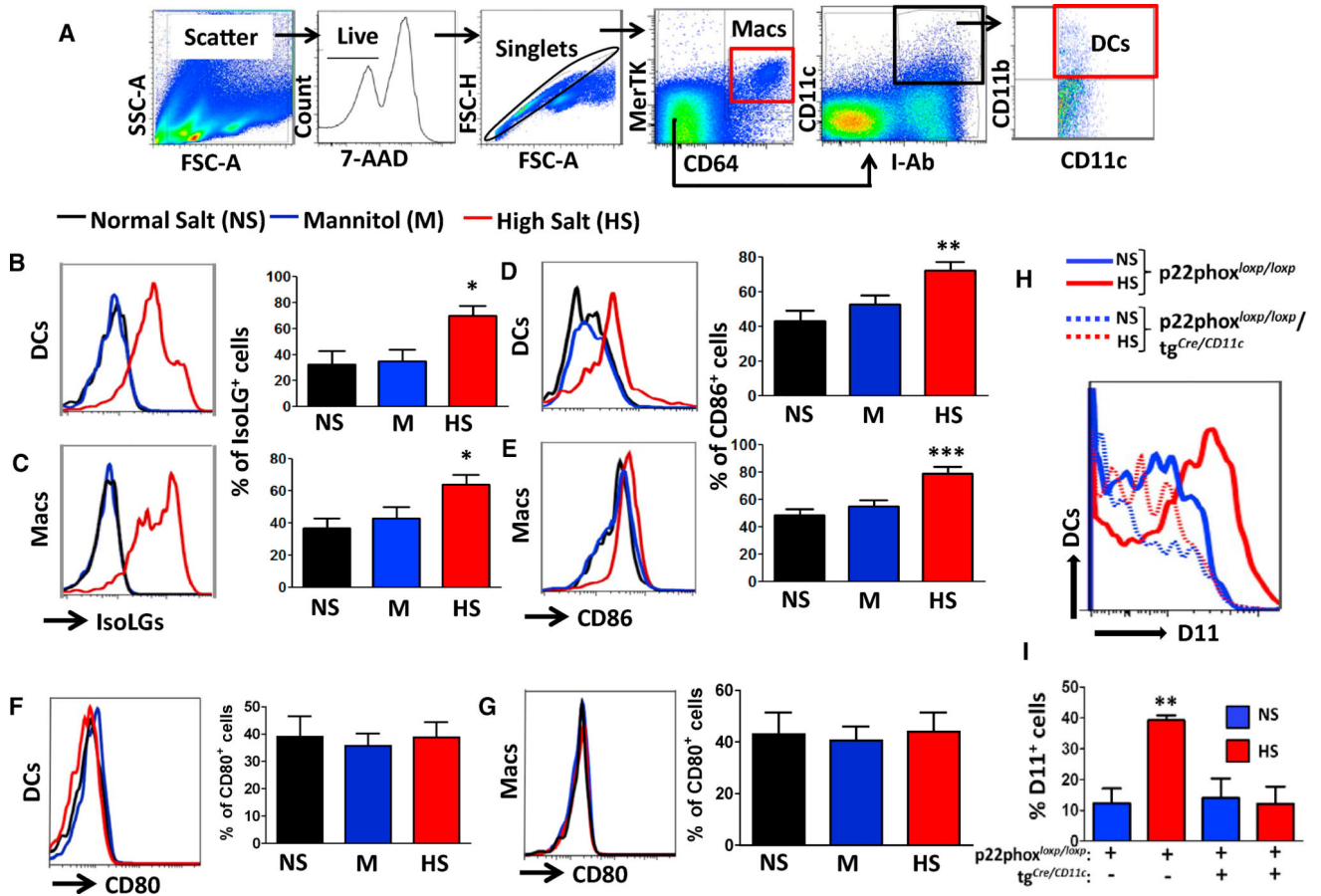


**Figure 3. Excess Salt Induces Formation of Immunogenic IsoLGs and Expression of B7 Ligands in Dendritic Cells and Macrophages**

Mouse splenocytes were cultured in normal-salt media (150 mM NaCl), high-salt media (190 mM NaCl), or normal-salt media with added mannitol (80 mM) as an osmotic control for 24 hr.

(A) Flow cytometry gating strategy to identify dendritic cells and macrophages.

(B and C) Flow cytometry representatives and average data showing intracellular staining for IsoLG-protein adducts in dendritic cells (B) and macrophages (C) using the single-chain antibody, D11 ScFv.

(D and E) Flow cytometry representatives and average data showing surface expression of CD86 in dendritic cells (D) and macrophages (E).

(F and G) Flow cytometry representatives and average data showing surface expression of CD80 in dendritic cells (F) and macrophages (G) ( $n = 5-6$ , \* $p < 0.05$ , \*\* $p < 0.01$ , \*\*\* $p < 0.001$  versus normal-salt control).

(H) Representative flow cytometry histograms showing the effect of salt on dendritic cells lacking the NADPH oxidase subunit p22<sup>phox</sup>.

(I) Average data showing the effect of salt on dendritic cells lacking the NADPH oxidase subunit p22<sup>phox</sup> ( $n = 6$ , \*\* $p < 0.01$ , expressed as mean  $\pm$  SEM).

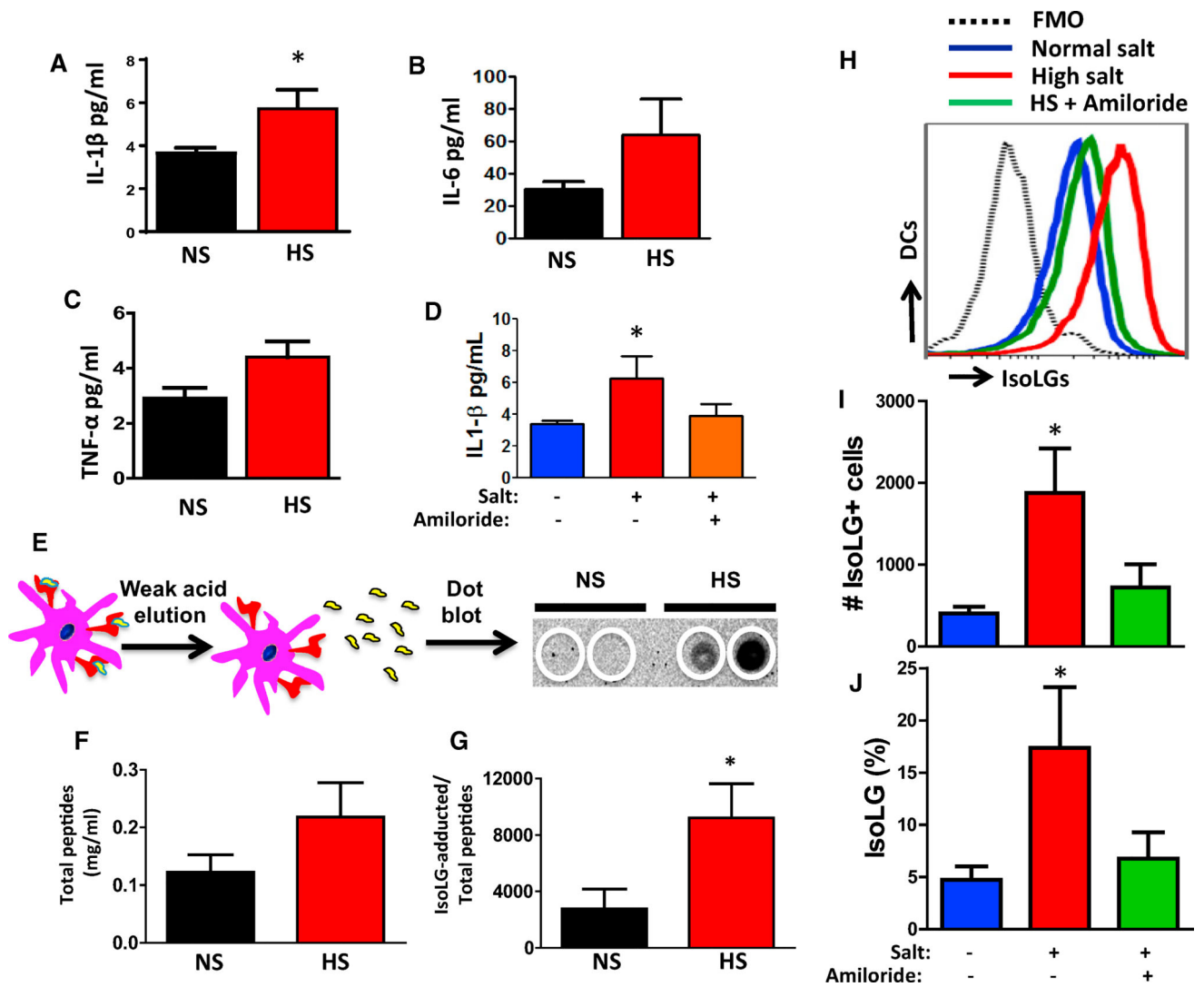


**Figure 4. Dendritic Cells Exposed to High Salt Have Increased Production of IL-1 $\beta$  and IsoLG-Adducted Peptides in Their MHC**

(A–C) Dendritic cells were isolated from spleens of mice, cultured in normal-salt or high-salt media and cytokines IL-1 $\beta$  (A), IL-6 (B), and TNF- $\alpha$  (C) were measured using a Luminex-based assay.

(D) Effect of amiloride on the high-salt-induced production of IL-1 $\beta$ .

(E) Surface peptides were eluted from dendritic cells treated with normal salt or high salt and dot blots were performed using the D-11 antibody.

(F) Total amount of peptides eluted.

(G) IsoLG-adducted peptides.

(H) Flow cytometry representative histogram showing the effect of amiloride on the high-salt-induced accumulation of IsoLG-adducted peptides in dendritic cells (FMO control is shown).

(I) Number of cells containing IsoLGs in normal-salt, high-salt, and high-salt + amiloride-treated dendritic cells.

(J) Percentage of cells containing isolevuglandins in normal-salt, high-salt, and high-salt + amiloride-treated dendritic cells (n = 5–10, \*p < 0.05 versus normal-salt control, expressed as mean ± SEM).

Author Manuscript

Author Manuscript

Author Manuscript

Author Manuscript

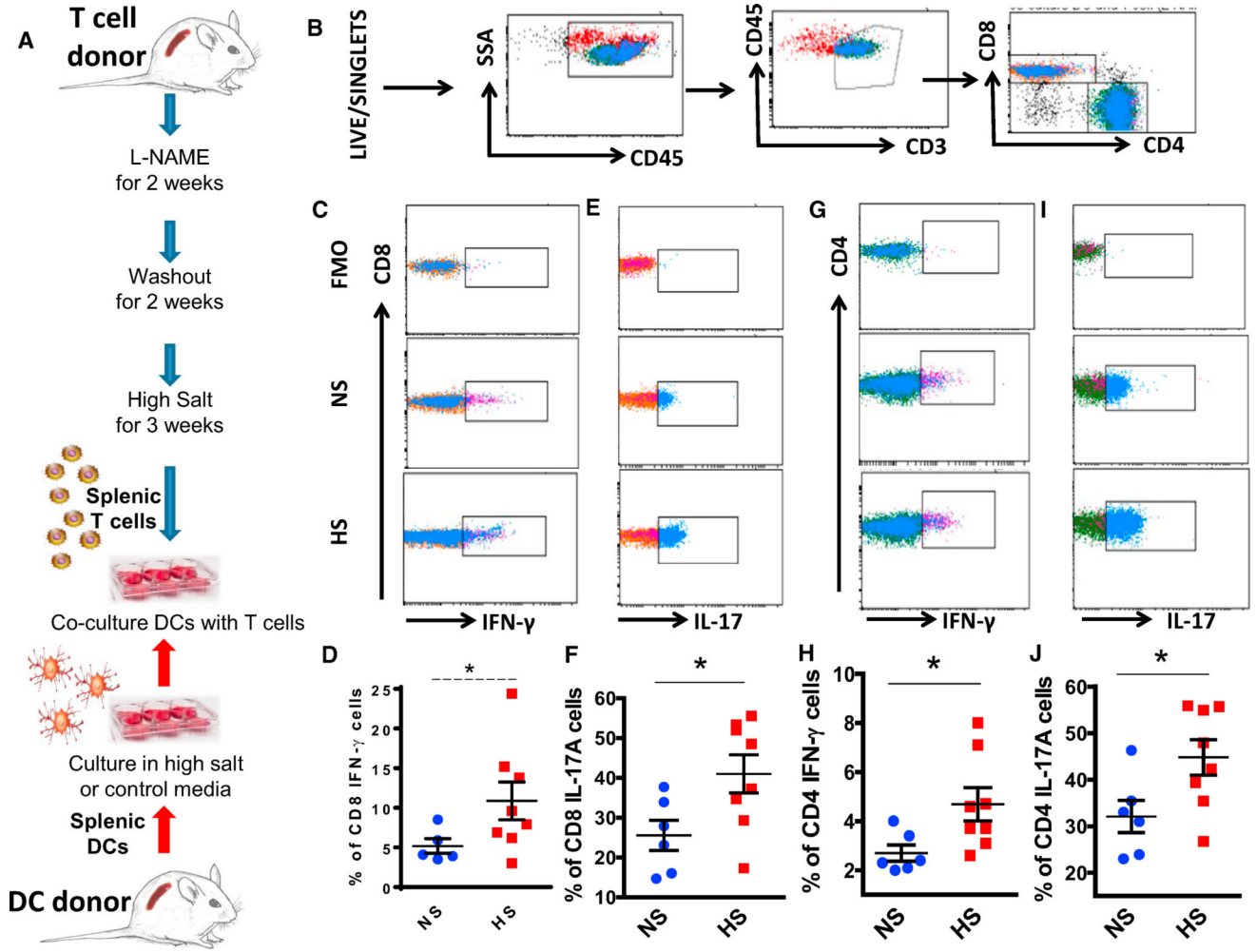


**Figure 5. Dendritic Cells Exposed to High Salt Induce Production of Pro-hypertensive Cytokines by Primed T Cells**

- (A) Experimental strategy where dendritic cells were cultured in normal or high-salt media and then co-cultured with T cells isolated from mice that were exposed to repeated hypertensive challenges.
- (B) Flow cytometry gating strategy to identify T cells subsets.
- (C) Flow cytometry representatives showing intracellular staining for IFN- $\gamma$  among CD8<sup>+</sup> T cells in response to DCs treated with normal salt and high salt.
- (D) Average data showing the effect of high-salt-treated dendritic cells on IFN- $\gamma$  production among CD8<sup>+</sup> cells.
- (E) Flow cytometry representatives showing intracellular staining for IL-17 among CD8<sup>+</sup> T cells in response to DCs treated with normal salt and high salt.
- (F) Average data showing the effect of high-salt-treated dendritic cells on IL-17 production among CD8<sup>+</sup> cells.
- (G) Flow cytometry representatives showing intracellular staining for IFN- $\gamma$  among CD4<sup>+</sup> T cells in response to DCs treated with normal salt and high salt.
- (H) Average data showing the effect of high-salt-treated dendritic cells on IFN- $\gamma$  production among CD4<sup>+</sup> cells.

(I) Flow cytometry representatives showing intracellular staining for IL-17 among CD4<sup>+</sup> T cells in response to DCs treated with normal salt and high salt.

(J) Average data showing the effect of high-salt-treated dendritic cells on IL-17 production among CD4<sup>+</sup> cells. The Flow-minus-one (FMO) gating controls are shown in the top panels (n = 5–8, \*p < 0.05 versus normal-salt control, expressed as mean ± SEM).

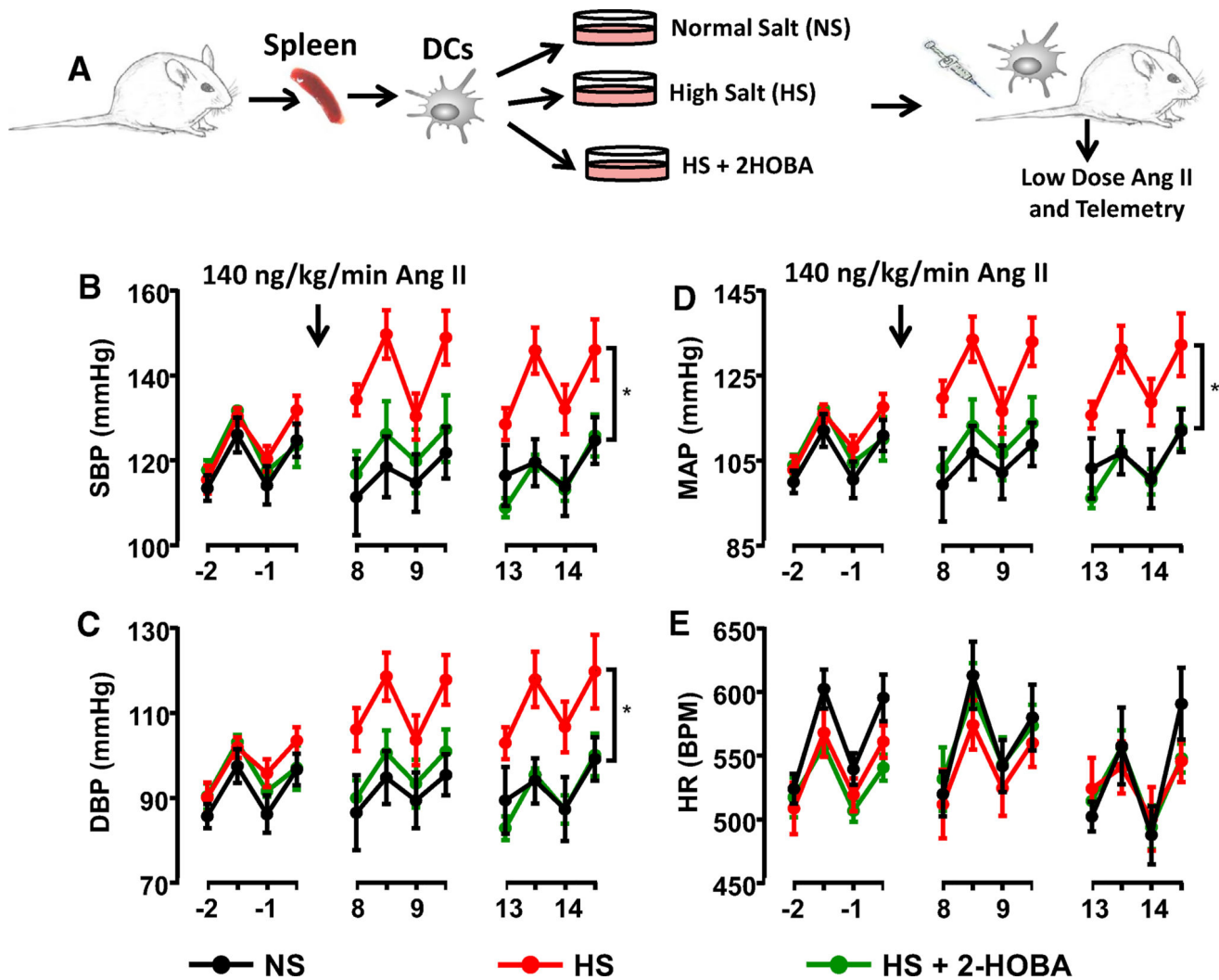


**Figure 6. Salt-Activated Dendritic Cells Sensitize Mice to a Normally Suppressor Dose of Angiotensin II, Leading to Hypertension**

(A) Dendritic cells were isolated from mouse spleens, cultured for 24 hr in normal salt, high salt, or high salt plus the isolevuglandin scavenger 2-HOBA and adoptively transferred into naive mice ( $10^6$  DCs per mouse) via intravenous injection. Two weeks later, osmotic mini-pumps were implanted subcutaneously to deliver a low dose of angiotensin II (140 mg/kg/hr).

(B–E) Systolic (B), diastolic (C), mean arterial blood pressure (D), and heart rate (E) were monitored using radio-telemetry ( $n = 5-6$ ,  $*p < 0.05$  versus normal-salt control, expressed as mean  $\pm$  SEM).